Brazilian Journal of Analytical Chemistry
Pre-publication – Accepted after peer review
doi: 10.30744/brjac.2179-3425.AR-122-2021

BrJAC

ARTICLE

Evaluation of a Lignin Bio-alkyd Resin for the Selective Determination of Molybdenum in Biological, Pharmaceutical, Fertilizer and Water Samples

Elhossein A. Moawed*, **Sara M. Ragab**, **Amira R. El-Shobaky**, **Maha A. El Hagrasy**

Chemistry Department, Faculty of Science, Damietta University, P.O. Box: 34517, Damietta, Egypt

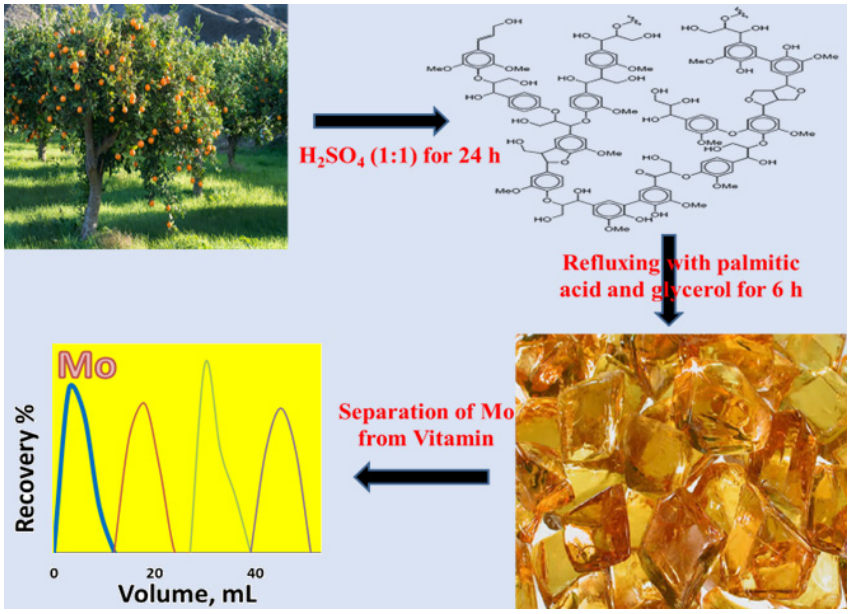

A lignin-based bio-alkyd resin (LA-Resin) was synthesized by the polycondensation reaction of lignin with a mixture of palmitic acid and glycerol. The LA-Resin was characterized using many techniques, including scanning electron microscopy, Fourier transform infrared spectroscopy, X-ray diffraction and thermal analysis. LA-Resin was proven to have graphitized structures with enhanced surface functional groups, showing a slightly basic character [pH of zero charge point (pH_{ZCP}) = 7.8]. It has a relatively better cation exchange capacity (0.70 mmol g^{-1}) in addition to the ability for physical adsorption. The performance of LA-Resin was assessed for the uptake of molybdenum (Mo), followed by spectrophotometric determination, applying both batch and column techniques. Elevated sorption percentages of Mo were observed in acidic medium H_2SO_4 (1.5 mol L^{-1}) in the presence of ascorbic acid (0.050 mol L^{-1}) and NH_4SCN (0.10 mol L^{-1}). The method was successfully applied to the separation and determination of Mo in mice liver, pharmaceuticals, water and fertilizer samples. Validation showed good recovery (96.6-99.6%), sensitivity (LOD, 0.9-4.0 µg L^{-1}), repeatability (RSD% ≤1.5%) and linearity (R^2 = 0.984), demonstrating a good quantitative performance of the method. Mo in all investigated samples regardless of different matrices were well-separated and detected, indicating that the method is sensitive enough to detect low concentrations of Mo even in small samples such as mice liver.

Keywords: Bio-alkyd resin, Molybdenum, Orange tree, Lignin, Pharmaceuticals

Cite: Moawed, E. A.; Ragab, S. M.; El-Shobaky, A. R.; El Hagrasy, M. A. Evaluation of a Lignin Bio-alkyd Resin for the Selective Determination of Molybdenum in Biological, Pharmaceutical, Fertilizer and Water Samples. *Braz. J. Anal. Chem.* (Forthcoming). http://dx.doi.org/10.30744/brjac.2179-3425.AR-122-2021

Submitted 15 January 2022, Resubmitted 31 March 2022, 2nd time Resubmitted 18 April 2022, Accepted 18 April 2022, Available online May 2022.

INTRODUCTION

Molybdenum (Mo) is an essential microelement for biological organisms due to its important role in maintaining several biological activities, enzymatic processes, and synthesis of proteins and nucleic acids.[1] Also, it is used for the regulation of body processes e.g., controlling digestion, eliminating harmful substances, reducing the activity of toxic compounds in the blood and suppressing cancer-causing agents.[2] Excess of Mo uptake results in severe gastroenteritis, decreased milk production, osteoporosis, and retarded growth. In addition, low Mo content affects adversely growth and may lead to neurological disorders and even early death. Mo also has a positive effect in the prevention of tooth decay.[3]

Mo was determined in various biological and pharmaceutical samples using different techniques.[4-7] The separation/spectrophotometric method is preferable, simple, inexpensive, and easy to handle.[8,9] In view of the very low concentration of Mo in environmental samples, it requires suitable methods for its preconcentration prior to its estimation.[10]

Adsorption is widely applied for the preconcentration and separation of diverse compounds including heavy metals. Bio-based sorbents are receiving great interest since they are environmentally friendly materials and have low to non-negative impact to environment. They, either in their pristine form or modified, have been extensively applied for the separation of different species regardless of their net charge.

Lignin is the most abundant natural aromatic biopolymer, it is produced as a waste product of the paper and pulp industry, and yet only a minute percentage is used for further refinement.[11] It contains various functional groups, such as ether linkages, aromatic hydroxyl, methoxy and aldehyde groups, making it appropriate for several modifications.[12] Functionalization of lignin would alter the chemical properties of the resulting material, which would offer enhanced sorption efficiency towards broader spectrum of pollutants. In addition, crosslinking of lignin can produce a more stable structure; hence, lignin would be a potential candidate for the preparation of different sorbents with distinctive characteristics.[13] The utilization of lignin not only provides potential sorbents, but also minimizes its impact, as a waste material, to the environment. Noteworthy drawbacks of lignin, however, are its brittle nature, along with its highly complex 3D structure, very low reactivity and its poor mechanical property. It is also a challenging task to recover lignin in a pure and clean form.[14] All of these would promote substantial challenges to its application. To overcome such drawbacks, lignin would be either incorporated into polymers, with relatively better properties, or chemically modified to produce materials with novel properties. Many studies have been performed to develop various lignin-based materials for different applications. Its composites were investigated for the removal cations and anions.[15] Also, it was produced in the form of microspheres and functionalized with amino groups for the removal of heavy metals.[16] In addition, the combination of lignin and surface-active layer was reported to be an effective approach for dye removal and heavy metal remediation as that found after the addition of reduced graphene oxide to lignin-poly(N-methylaniline).[17]

Alkyd resins (ARs) are eco-friendly highly branched polymers with a polyester backbone mainly developed for coating purposes[18] and recently were applied for the removal of contaminants.[19] They are prepared with abundant and bio-based resources by the polycondensation (esterification) of three types of monomers, which are polyhydric alcohols, polybasic acids and fatty acids.[20] ARs are inexpensive, thermally stable, soluble in organic solvents, have the ability to disperse pigments and fillers and have good adherence to different surfaces.[21] Having a molecular structure consists of hydroxyl groups, unsaturated double bonds, ester groups and carboxyl groups, enables its modification by the reaction with various materials, resulting in novel materials with enhanced properties.[22]

In this study, taking into consideration the necessity of green transition to address the global warming crisis, a simple, environmentally benign, and cost-effective sorbent was developed by the reaction of oxidized lignin, separated from orange tree wood, as a source of carboxylic groups, with a mixture of palmitic acid and glycerol to synthesis LA-Resin, via polycondensation reaction, for the purpose of selective separation of Mo. LA-Resin was characterized by scanning electron microscopy (SEM), Fourier transform infrared spectroscopy (FTIR), ultraviolet and visible spectroscopy (UV-Vis), X-ray diffraction analysis (XRD) and thermogravimetric analysis (TGA). LA-Resin was evaluated for the uptake of Mo from acidic solutions,

followed by spectrophotometric detection. In addition, adsorption isotherms, the corresponding kinetics, thermodynamic analysis, interference studies, column studies, stripping and reusability of the sorbent were also carried out. The developed quantitative method was validated in terms of addition and recovery, limits of detection and quantitation, linearity, repeatability, and selectivity. The method was applied for the preconcentration and separation of Mo from mice liver, pharmaceutical, water and fertilizer samples.

MATERIALS AND METHODS

Apparatus

The crystal structure of LA-Resin (XRD patterns) was investigated using an X-ray diffractometer (D8-Brucker Model) equipped with Cu Kα radiation (λ = 1.54 Å). The surface morphology of LA-Resin was analyzed using scanning electron microscope (SEM, JEOL model JSM-6510LV, USA). FTIR studies were carried out using a JASCO-410 spectrometer (JASCO, Easton, MD). A UV–Vis spectrophotometer (JASCO, V-630 UV-Vis Spectrophotometer, Japan) was employed for absorbance measurements. Thermogravimetric analysis (TGA), differential thermal analysis (DTA) and differential scanning calorimetry (DSC) were carried out by DSC-TGA device model (SDTQ 600, USA) under N_2 atmosphere with a heating rate of 10 °C/min (29-1000 °C).

Reagents and materials

All chemicals were of analytical grade reagents and used without further purification. Molybdenum (Mo) stock solution (1000 mg L^{-1}) was prepared by dissolving $(NH_4)_6Mo_7O_{24}.4H_2O$ (Merck) in doubly distilled water (DDW). Experimental solutions for adsorption and analysis were freshly prepared by diluting Mo stock solution with DDW. Nitric acid (65%, m/v), Sulfuric acid (98%, m/v) and ammonium hydroxide (29%, m/v) (Fluka) were used. Ascorbic acid (AA), ammonium thiocyanate, palmitic acid and glycerol were purchased from Sigma Aldrich.

Orange tree wood was obtained from local area in Damietta, Egypt. Wood samples were washed thoroughly with distilled water to remove dust and other impurities. These were cut into small pieces and dried in an oven at 105 °C, left to cool followed by grinding and sieving. For separating lignin, a 100 g sample of the powder was treated with a volume of 500 mL H_2SO_4 (1:1) for 24 h under stirring to remove the polysaccharide fraction. The acid-insoluble lignin residue was filtered, washed thoroughly with distilled water until a filtrate with a neutral pH value was obtained. For preparing oxidized lignin, solid lignin was treated with 100 mL of 0.1 mol L^{-1} $KMnO_4$ in 0.1 mol L^{-1} H_2SO_4 for 3 h at room temperature then filtered, washed thoroughly with distilled water and dried at 105 ºC. A 15 g of the as prepared material was refluxed with a mixture of 85 g of palmitic acid, and 30 g of glycerol for 6 h. The final product (LA-Resin) was separated, washed with distilled water, methanol and dried at 25 ºC.

Recommended procedures

Batch method was performed by mixing 0.10 g of LA-Resin with 25 mL of Mo(VI) solution (0.083 mmol L^{-1}) containing H_2SO_4 (0.1–2.0 mol L^{-1}), ascorbic acid (0.01–0.1 mol L^{-1}) and NH_4SCN (0.05–0.2 mol L^{-1}). The mixture solution was then shaken for 1 h at room temperature. After equilibrium, the solution samples were filtered and the concentration of the remaining and recovered Mo from the LA-Resin was determined spectrophotometrically as thiocyanate complex at λmax 457 nm (Figure 1S). Kinetic studies were conducted with a concentration of (0.083 mmol L^{-1}) molybdenum solution, and Mo uptake was carried out at different time intervals (1 - 120 min). The uptake percentage (E%) and equilibrium adsorption capacity of Mo (qe, mg/g) were calculated according to Equations (1) and (2).

$$E\% = 100\ ((C_0 - C_e)/C_0) \quad (1)$$

$$qe = V(C_0 - C_e)/m) \quad (2)$$

where, C_0 and C_e (mmol L^{-1}) are the initial and equilibrium Mo concentrations, respectively, V (L) is the solution volume, and m (g) is the dry mass of LA-Resin.

Dynamic method was performed using a 1.5 cm diameter glass column (35 cm length). The glass column was carefully loaded with a water slurry of LA-Resin material (10 g) to a bed height of 15 cm. Voids in the column bed were completely eliminated. Feed solutions of Mo, containing H_2SO_4 (1.5 mol L^{-1}), AA (0.050 mol L^{-1}) and NH_4SCN (0.10 mol L^{-1}) were passed through the column at a predetermined rate. Eluent solution contained 0.050 mol L^{-1} NH_4OH. The feed solution flow and elution rates were both set to 1–5 mL min^{-1}. Fractions of the solution (3 mL each) were collected then analyzed.

Pharmaceuticals used in this study are Ferrotron: Fe 15 mg; Cu 0.9 mg; Zn 11 mg and Mo 45 µg, Vitamix plus: Cu 2 mg; Fe 9 mg; Mn 5 mg and Mo 30 µg, Phara ferro 27 tablets: Cu 1 mg; Fe 30 mg; Zn: 2.5 mg; Mo: 15 µg (Nasr city, Egypt), and Octatron multivitamins capsules: Mo: 45 µg; Zn: 11 µg; Se: 55 µg; (Giza, Egypt). To prepare drug solutions. To prepare drug solutions, capsules or tablets, containing the desired Mo concentration, were dissolved in concentrated nitric acid and gently evaporated till dryness, then the solid residue was dissolved in DDW acidified with drops of nitric acid then quantitatively transferred into 25 mL measuring flasks, containing H_2SO_4 (1.5 mol L^{-1}), AA (0.050 mol L^{-1}) and NH_4SCN (0.10 mol L^{-1}) then completed to the mark with DDW.

Mice liver samples, containing pre-determined concentration of Mo, were kindly provided by Zoology Department, Faculty of Science, Damietta University. A 0.225 g sample of liver tissue was digested in a minimal volume of aqua regia and heated to ensure complete digestion. The digested was then dissolved with DDW and treated the same way as drug samples.

Water samples, collected from Damietta (Egypt), including River Nile, seawater, and industrial wastewater were filtered using a Millipore 0.45 µm pore-size membrane and kept in polyethylene bottles. The water sample was spiked with Mo(VI) solution (1 µg L^{-1}) and then determined as a molybdenum thiocyanate complex. Fertilizer sample (micro zein fertilizer), containing Zn: 2.4%; Fe: 2.4%; Mn: 2.4%; Cu: 0.6%; B: 0.6%; Mo: 0.06%; and S: 3.2% W/V (Unikim Tekstil Boyalarive, Turkey) was treated the same way as those of the pharmaceuticals.

The reusability of LA-Resin was explored for batch and continuous modes by following consecutive adsorption/desorption cycles. After each cycle, Mo was completely desorbed using 0.050 mol L^{-1} NH_4OH, followed by a through rinsing with distilled water until a neutral supernatant was acquired. Subsequently, after drying only for batch method, the same adsorbent mass was recycled under the aforementioned optimum adsorption experimental conditions.

RESULTS AND DISCUSSION

Characterization of LA-Resin

Of the advantages of LA-Resin, noticed during experimentation, is that it required very short time to dry and it was generally much easier to handle and to be separated. To assist the homogeneous dispersion of lignin into the alkyd resin matrix, lignin was oxidized to ensure the production of excess carboxylic groups to react with the alkyd formulation through a condensation reaction. SEM was used to compare between the surface morphology of lignin and that of LA-Resin. SEM micrographs, at magnifications of 3,000x and 5,000× of lignin show a bulk structure with wrinkled surface (Figure 1A, 1B). Whereas those of LA-Resin (Figure 1C, 1D) are completely different, they present prominent changes in the texture they show it has a multi-layered microstructure and contain many cavities with different sizes. Figures 1C and D illustrate interconnected well-organized sheets, with no visible boundaries between the mixture components and lignin could be no longer recognized, suggesting that lignin was completely well dispersed and integrated into the alkyd[23] formulation to produce LA-Resin. These observations demonstrate the successful preparation of LA-Resin

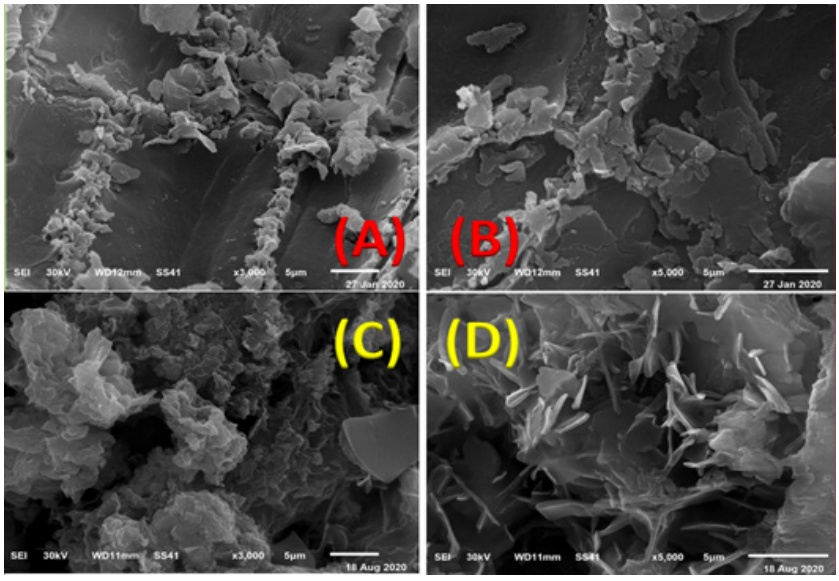

Figure 1. SEM micrographs of lignin (A, B) and LA-Resin (C, D) at magnifications of 3,000 and 5,000×.

FTIR was used to identify the chemical structure and functional groups of lignin, A-Resin and LA-Resin. The FTIR spectrum of lignin (Figure 2) shows a broad absorption band at 3729-2981 cm^{-1} which can be assigned to the stretching of phenolic and aliphatic -OH groups. Bands at 2923 cm^{-1} and 2855 cm^{-1} are ascribed to the C–H stretching of methylene and methyl groups, respectively. The characteristic bands located at 1511 and 1461 cm^{-1} correspond to the aromatic skeleton in lignin. These bands are nearly similar of the organosolv lignin.[24,25] The band at 1631 cm^{-1} is attributed to –C=O stretching of carboxyl groups conjugated with the aromatic ring. While the FTIR spectrum of A-Resin (Figure 2S), a broadband appeared from 3721 to 3103 cm^{-1} was assigned to OH group. Several sharp peaks were also observed at 2919, 2848 cm^{-1} (uCH), 1772-1565 cm^{-1} (uCO) and (uC=C) which characterize the matrix of A-Resin. All these band frequencies were shifted in the LA-resin spectrum (Figure 2) to 2797–3622, 2918, 2849, and 1556 cm^{-1}. In addition, two new sharp peaks developed at 1738 and 1268 cm^{-1}, which correspond to the –C=O and –COO stretching and the band at 1631 cm^{-1} was absent. It can be observed that most of the peaks of LA-resin are identical to those of alkyd resin. All these characteristic absorption bands support the formation of AR in the presence of lignin to obtain the LA-Resin.

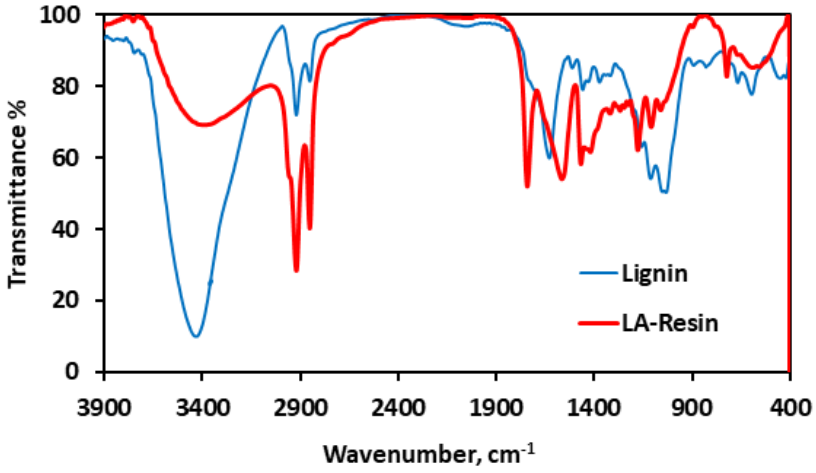

Figure 2. FTIR Spectra of lignin and LA-Resin.

Also, electronic spectra of solid-state lignin, A-Resin and LA-Resin, recorded in the range of ~ 200–400 nm (Figure 3S), reveal that lignin absorbs UV radiation very strongly below 215 nm and A-Resin at 373 nm. Whereas LA-Resin does not absorb below 290 nm and it has two distinctive sharp peaks at ~ 300 and 340 nm.

Of great importance to carbonaceous materials is the acid-base behavior of the surface functional groups and the value of pH_{zcp}, at which the net surface charge is zero. The surface acidic and basic functional groups of lignin and LA-Resin obtained from Boehm titration are reported in Table I. The results show that the total acidic and basic groups of LA-Resin are 1.48 and 1.62 mmol g^{-1}, respectively, which are greater than those of lignin (1.25 and 0.20 mmol g^{-1}, respectively). The decrease of the amount of carboxylic group from 0.63 to 25 mmol g^{-1} is due to it reacting with a glycerol molecule. The ratio of reacted lignin and incorporated lignin is the following 0.38: 0.25 (1.5:1). As evident, the value of basic functionalities of LA-Resin are relatively greater than that of the acidic one, rendering the surface slightly basic which was further indicated pHzcp measurements.

Figure 4S shows pH_{zcp} curves of lignin and LA-Resin. The estimated values are 3.0 and 7.8 for lignin and LA-Resin, respectively. These results are in accordance with the determined acidic and basic sites and supports the better performance of LA-Resin to remove different species regardless of their charge under any pH value. It is evident that the surface chemistry of LA-Resin is greatly altered compared to that of lignin in terms of enhanced acidic and basic functional groups.

Table I. Acidic and basic sites of sorbents

Sorbent	Basic Sites, mmol g^{-1}	Acidic Sites, mmol g^{-1}		
		Phenolic	Carboxylic	Lactonic
Lignin	0.20	0.15	0.63	0.47
LA-Resin	1.62	0.53	0.25	0.70

To investigate further the properties of the surface of LA-Resin, Iodine number (I_2 No) and methylene blue value (MB value) were determined. I_2 No would indicate the adsorption process of the sorbent while MB value implies the cation exchange ability. The I_2 No and MB value of lignin and LA-Resin are 1.6, 1.5, 0.6, and 0.7 mmol g^{-1}, respectively (Table II). In addition, electrical conductivity measurements were performed (σ). The values of σ of lignin and LA-Resin are 7×10^{-12} and 2×10^{-11} Ω^{-1} m^{-1}, respectively (Table II). This result signifies the very low electrical conductivities of both materials.

Table II. Iodine number and methylene value of sorbents

Sorbent	Iodine number mmol g^{-1}	Methylene blue value mmol g^{-1}	Electrical conductivity Ω^{-1} m^{-1}
Lignin	1.6	0.6	7×10^{-12}
LA-Resin	1.5	0.7	2×10^{-11}

Thermal properties of lignin and LA-Resin were evaluated using TGA, and DSC analysis (Figure 5S). These curves indicate two steps of thermal decomposition for both materials. The weight loss at initial stage until ~100 °C, due to loss of adsorbed water, for lignin and LA-Resin are 21.2, and 5.9%, respectively. At the second step, a weight loss of 39.0, and 74.1% is observed at 104-1000 °C, and 111-1000 °C for lignin and LA-Resin, respectively. The total weight loss of LA-Resin (80%) was higher than that of lignin (60.2%) which resulted from the decomposition of the alkyd polymer. While ≥ 90% of the weight loss for A-Resin was at 442 °C.[26]

A powder XRD study was performed to investigate the crystallographic nature of lignin (Figure 6S) and LA-Resin (Figure 3). The main characteristic feature noticed in both patterns is the presence of a broad diffraction peak at 2θ = 20–30° which, corresponds to the (002) plane of the graphitized structures.

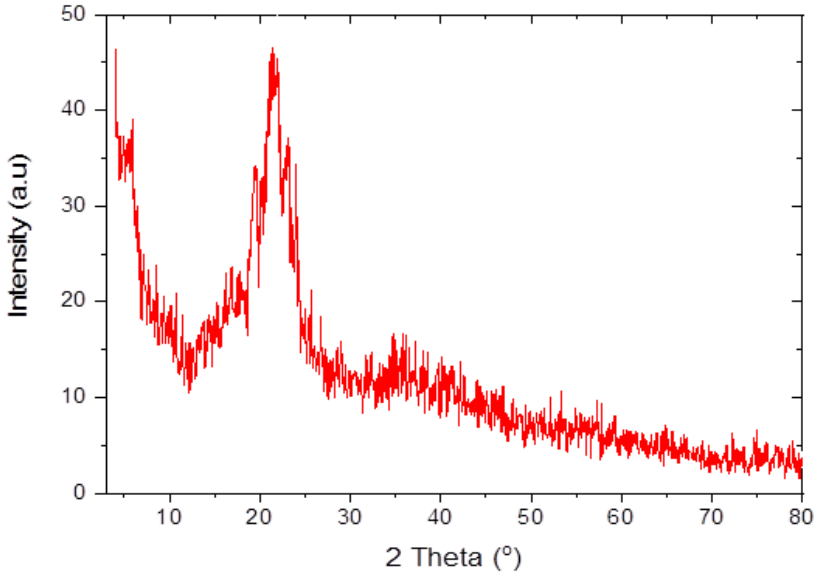

Figure 3. XRD pattern of LA-Resin.

Sorption of molybdenum ions

The sorption percentages of Mo from thiocyanate solution were investigated in an acidic medium (0.1–2.0 mol L^{-1} H_2SO_4), ascorbic acid (0.01–0.1 mol L^{-1}), ammonium thiocyanate (0.05–0.2 mol L^{-1}) and different weight of LA-Resin (0.05–0.2 g) (Figure 4). It was found that the optimum conditions for the sorption of Mo are 1.5 mol L^{-1} H_2SO_4, 0.06 mol L^{-1} ascorbic acid, 0.1 mol L^{-1} NH_4SCN and 0.1 g of LA-Resin.

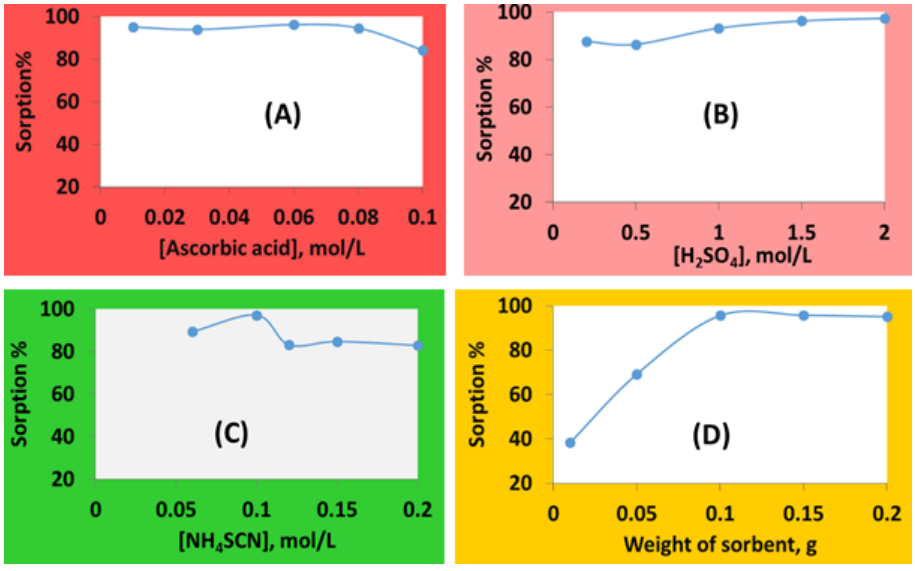

Figure 4. Conditions of the extraction of molybdenum from aqueous solution.

Mo adsorption onto LA-Resin occurred very rapidly within the first 5 min at which almost 75% of Mo was adsorbed. The adsorption rate decreased significantly after 30 min, which could be attributed to the decrease of adsorption reactive sites, available for Mo adsorption, then equilibrium was attained after 60 min. Consequently, 60 min was chosen as the optimum contact time. Pseudo-first-order (PFO) and pseudo-second-order (PSO) models were used to evaluate the adsorption kinetics. The results (Table 1S,

2S) suggest that Mo adsorption is better described by the PSO (R^2 = 0.997, Figure 7S), with a qe value almost equal to that of the experimental, kinetic model rather than PFO (R^2 = 0.750, Figure 7S). This result would indicate that Mo adsorption onto LA-Resin follows a chemisorption mechanism by sharing or replacing electrons between LA-Resin and Mo.

The adsorption capacity of LA-Resin was investigated by adsorption isotherms. As shown in Figure 8S, the uptake of Mo onto LA-Resin increases with the increase of concentration until a plateau is reached (q_{max} = 31.7 mg g^{-1}). The experimental data were then fitted by the Langmuir and Freundlich models to determine whether the adsorption process was a monolayer or a multilayer adsorption. The obtained results (Table S1) indicate that compared to Freundlich model (R^2 = 0.860, Figure 8S), Langmuir model (R^2 = 0.920, Figure 8S) is a good fit to the experimental data, suggesting a mono-molecular layer sorption, with a maximum monolayer sorption capacity of 39.20 mg g^{-1}, of Mo as well as a homogeneous distribution of active sites on the LA-Resin surface. Table 4S illustrates the adsorption capacities of some sorbents, revealing the good sorption capacity of LA-Resin.

The effect of temperature (25–60 °C) on the sorption of Mo ions using LA-Resin was studied. It was found that the sorption of Mo ions very slightly increased with increasing temperature. The calculated thermodynamic parameters are Gibbs's free energy (ΔG), enthalpy (ΔH), and entropy (ΔS) (Figure 9S, Table 5S, 6S). ΔH is 21.6 kJ mol^{-1}, the positive value reveals that the extraction of Mo ions by LA-Resin is endothermic. ΔG is -19.20 kJ mol^{-1}, indicating a spontaneous sorption process and ΔS is 137 J K^{-1} mol^{-1}.

Mechanism of Mo adsorption onto LA-Resin

LA-Resin has a relatively weak basic character, where the activity of total acidic and basic groups is 1.48 and 1.62 mmol g^{-1}, respectively, which was further indicated by a pH_{ZCP} value of 7.8. It has a good ability to accommodate Mo through different mechanisms since it has a cation exchange capacity of 0.70 mmol g^{-1} in addition to the ability for physical adsorption (I_2 No = 1.5 mmol g^{-1}) as also indicated from SEM images. Under the optimum conditions, Mo ions would be present as $[Mo(SCN)_6]^-$ and the surface of LA-Resin would be positively charged due to the protonation of the basic functional groups (solution pH < pH_{ZCP}). Accordingly, adsorption would firstly start as a result of the electrostatic attraction between the protonated LA-Resin surface and the negatively charged Mo thiocyanate complex and this would be the initial driving force to bind Mo to the sorbent surface. Afterwards, inner sphere complexation might have happened, as indicated by kinetic studies, which is the most important mechanism for Mo adsorption where it could be adsorbed into LA-Resin surfaces through coordination with functional groups (Figure 5).

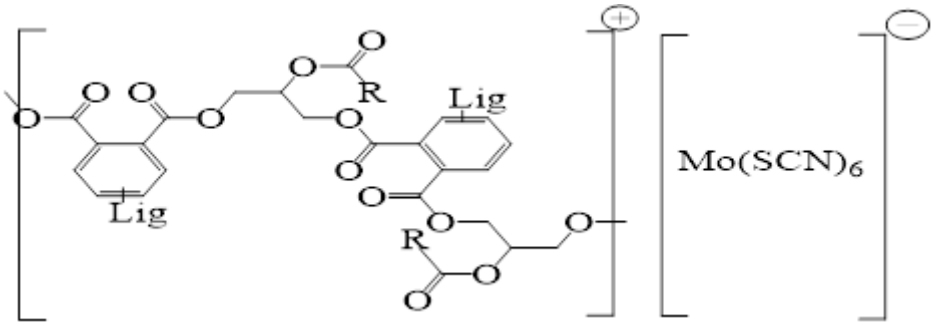

Figure 5. A mechanism scheme for the sorption of Mo onto LA-Resin.

Effect of foreign ions

The effect of the presence of different ions on the adsorption of molybdenum (200 µg) onto LA-Resin, using batch mode, was examined (Figure 10S). Ions such as Na^+, K^+, Mn^{2+}, Ni^{2+}, Pb^{2+}, Co^{2+}, Zn^{2+} and Ca^{2+} (1000 µg) had almost no interference (< 2%). However, Sb^{3+} and Fe^{3+} (1000 µg) caused noticeable interference (16-17%). The addition of either 1mL of 0.1 M citric acid or excess ascorbic acid solution eliminated such interference.

Column studies

The extraction and recovery of Mo ions were tested using a LA-Resin-loaded column (35 cm long and 1.5 cm in diameter contained 10 g of LA-Resin with bed height 15 cm). It was found that Mo ions were completely adsorbed under the optimized conditions and were eluted with 10-15 mL of 0.05 mol L^{-1} NH_4OH solutions at 1-5 mL min^{-1} (Figure 6). To investigate the effect of sample loading and eluent flow rates on Mo retention and recovery, either feed solutions of Mo, under the optimized experimental conditions, or eluent solutions (0.050 mol L^{-1} NH_4OH) were passed through the column at different flow rates varying from 1–5 mL min^{-1}. The flow rate of sample loading in the investigated range did not show any difference (data not shown) so, a flow rate of 1 mL min^{-1} was chosen for further experiments. According to the results shown in Figure 6, Mo species were eluted completely under the investigated range however, a better-resolved peak was obtained at eluent flow rate of 1 mL min^{-1}, accordingly, it was further applied for eluting Mo species. Preconcentration of Mo from water samples was investigated. Solutions of 100 µg of Mo ions in up to 500 mL of water samples were passed through the LA-Resin column (1 mL min^{-1}). The elution of Mo ions from the LA-Resin column was carried out by 10 mL NH_4OH (0.05 mol L^{-1}) solution then the eluates were determined.[27] The results show that the recovery percentages are about 100% with a preconcentration factor of up 50.

Capacity of the LA-Resin column was calculated by percolating it with Mo solution (0.10 mg mL^{-1}) at a flow rate of 1 mL min^{-1}. Breakthrough curves were obtained by measuring the content of Mo ions in 5 mL collected fractions from the effluent (Figure 11S). The breakthrough point is reached at a volume of 100-480 mL, the breakthrough capacity was 36.5 mg L^{-1}.

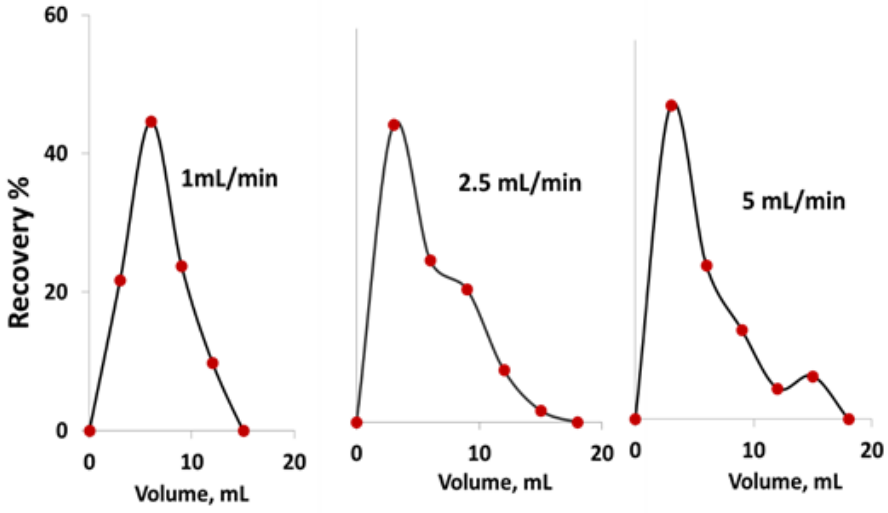

Figure 6. Effect of eluent flow rate on the recovery of molybdenum from LA-Resin column.

Regeneration of LA-Resin

The regeneration experiments were carried out to evaluate the reusability of AL-Resin. Based on the point that the adsorption of Mo onto LA-Resin took place in acidic medium, Mo desorption was tested in basic solution. The LA-resin material was affected at pH ≥ 12 using NaOH solution (Figure 12S) and not effect with ammonia solution. Therefore, the best eluent examined was NH_4OH with a concentration of 0.05 mol L^{-1} at 25 ºC for 12 h. After five cycles of regeneration, in batch mode, the adsorption capacity was unchanged as well as the removal efficiency. For column experiments, one column was conducted through the whole experiment for more than 10 cycles of sorption/desorption and it kept its performance unchanged. These results suggest that LA-Resin is not only a selective material for Mo at the investigated operating conditions but also could be an efficient adsorbent for the removal of Mo from different matrices.

Analytical performance of the proposed method

A calibration curve for Mo was obtained, applying the optimized preconcentration method. The linear range was obtained for a concentration range near the limit of quantification (LOQ) up to 15 mg L^{-1}, with R^2 value of 0.984. The analytical sensitivity was assessed by the limits of detection (LOD) and limits of quantitation (LOQ) for the extraction and recovery of Mo from the investigated biological and pharmaceutical samples using LA-Resin columns (Table III). The values of LOD and LOQ are in the range of 0.9-4.0 and 2.9-13.4 µg L^{-1}, respectively (n = 5) which indicate the higher sensitivity of Mo determination by LA-Resin columns compared to other reported results. The accuracy and precision for the determination of Mo using LA-Resin in real samples were investigated by analyzing spiked samples. Table IV shows the results of extraction and recovery of Mo from mice liver and pharmaceutical samples. The high recoveries (96.6–99.6%) of Mo along with their lower values of RSD% (0.3-1.5%, n = 5) reflect the good accuracy and precision of the proposed method.

Table III. Detection limit of molybdenum

Samples	LOD, µg L^{-1}	LOQ, µg L^{-1}
Liver mice tissue	2.5	8.4
Vitamix plus capsule	3.2	10.6
Octatron capsule	1.7	5.7
Ferrotron capsule	4.0	13.4
Phara ferro 27 tablet	0.9	2.9

Table IV. Determination of molybdenum in real samples

Samples	Added, µg	Found, µg	Recovery, %	RSD, %
Liver mice tissue	105	104.6	99.6	0.9
Vitamix plus capsule	90	88.8	98.7	1.2
Octatron capsule	90	89.5	99.5	0.5
Ferrotron capsule	90	86.9	96.6	1.5
Phara ferro 27 tablet	100	98.1	98.1	0.3

Preconcentration and recovery of Mo from real samples

Figure 7 shows chromatographic separation of Mo from other metals in Mo-containing pharmaceuticals, Ferrotron and Vitamix plus, on LA-Resin-packed columns. The elution of Mo was carried out at a flow rate of 1.0 mL min^{-1} using NH_4OH (0.05 mol L^{-1}), then the concentrations were determined spectrophotometrically. Mo ions were completely eluted from LA-Resin columns with a recovery percentage of 100% at the first 12 mL of NH_4OH solution. The resolution factors (Rs) for the separation of Mo from Cu ions in Vitamix plus and Ferrotron samples, calculated by the following equation: $Rs = 2(V_2 – V_1)/(W_1+W_2)$ are 1.1 and 1.4, respectively. These results considerably suggest that LA-Resin columns have the potential, under the operational conditions, for the separation of Mo from different matrices with good resolution and could be completely recovered from real samples.

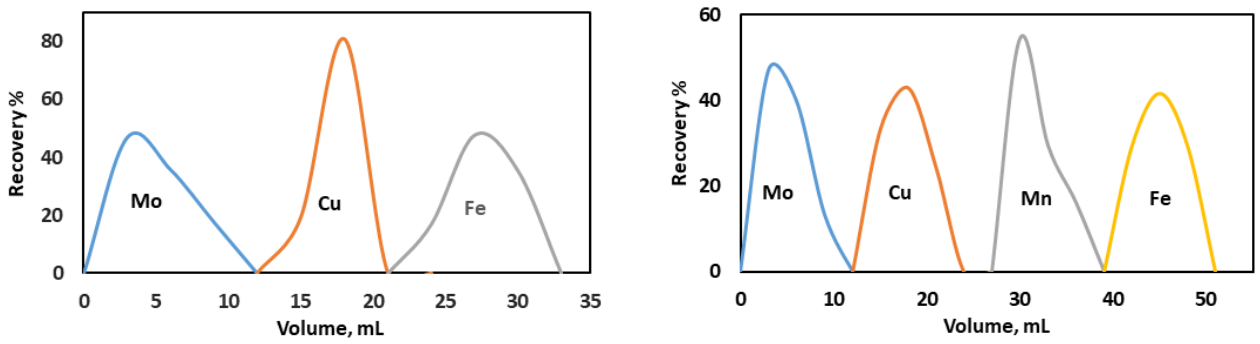

Figure 7. Chromatographic separation of molybdenum from pharmaceutical samples.

For the determination of Mo–bound in biological samples, using the mice liver as a model, the digest of mice liver samples, containing pre-determined concentration of Mo, were treated the same way as drug samples. The results (Table IV) show that the recovery percentage of Mo is 99.6% (RSD = 0.90%, n = 5).

LA-Resin column was applied for the extraction of Mo from water samples, namely, River Nile, seawater and industrial wastewater. Mo-spiked water samples, treated under the optimized conditions, were allowed to pass through the LA-Resin columns at a flow rate of 1 mL/min. The elution of Mo from the LA-Resin column was carried out by NH_4OH (0.05 mol L^{-1}) solution and the amount of Mo in the eluates were determined by the recommended method. The results show that the average recovery percentages of Mo are 100% (RSD = 0.00%, n = 5). Therefore, LA-Resin column could be applied for the recovery of Mo from different water samples. In addition, Mo content in micro zein fertilizer was assessed by LA-Resin column. The results show that the recovery percentage of Mo (60 µg) is 100% (RSD = 0.76%, n=5).

CONCLUSION

LA-Resin was synthesized and characterized by many techniques. The sorbent has a relatively weak basic character, where the total acidic and basic groups are 1.5 and 1.6 mmol g^{-1}, respectively. It has a good ability to accommodate sorbate species through different mechanisms since it has a cation exchange capacity of 0.7 mmol g^{-1} in addition to the ability for physical adsorption (I_2 No = 1.5 mmol g^{-1}). The sorbent showed, under the optimum conditions, that the uptake of $[Mo(SCN)_6]^-$ complex onto the positively charged LA-Resin most probably took place through the formation of ion-associate complex. Kinetic studies revealed that the removal of Mo follows a chemisorption mechanism by sharing or replacing electrons between LA-Resin and Mo. LA-Resin has a homogeneous distribution of active sites to accommodate a mono-molecular layer of Mo (q_{max} = 31.7 mg g^{-1}) as indicated by sorption isotherm studies. Mo ions were desorbed effectively using an aqueous solution of 0.05 mol L^{-1} NH_4OH. A LA-Resin-column was tested for the uptake and elution of the Mo and the recovery was almost 100% suggesting a good efficiency of LA-Resin to the chromatographic separation. The reusability experiment indicated that LA-Resin is not only a selective material for Mo at the investigated operating conditions but also is an efficient and cost-effective adsorbent for the removal of Mo from different matrices.

Conflicts of interest

The authors certify that they have NO affiliations with or involvement in any organization or entity with any financial interest (such as honoraria; educational grants; participation in speakers' bureaus; membership, employment, consultancies, stock ownership, or other equity interest; and expert testimony or patent-licensing arrangements), or non-financial interest (such as personal or professional relationships, affiliations, knowledge or beliefs) in the subject matter or materials discussed in this manuscript.

Acknowledgements

The authors gratefully acknowledge research support from Damietta University and the Chemistry Department, Faculty of Science, Damietta University, Egypt.

REFERENCES

(1) Janani, I.; Lakra, R.; Kiran, M. S.; Korrapati, P. S. Selectivity and sensitivity of molybdenum oxide-polycaprolactone nanofiber composites on skin cancer: Preliminary in-vitro and in-vivo implications. *J. Trace Elem. Med. Biol*. **2018**, *49*, 60–71. https://doi.org/10.1016/j.jtemb.2018.04.033

(2) Ellingsen, D. G.; Chashchin, M.; Berlinger, B.; Fedorov, V.; Chashchin, V.; Thomassen, Y. Biological monitoring of welders' exposure to chromium, molybdenum, tungsten and vanadium. *J. Trace Elem. Med. Biol*. **2017**, *41*, 99–106. https://doi.org/10.1016/j.jtemb.2017.03.002

(3) Li, W.; Dong, X.; Zhu, L.; Tang, H. Highly selective separation of Re(VII) from Mo(VI) by using biomaterial-based ionic gel adsorbents: Extractive adsorption enrichment of Re and surface blocking of Mo. *Chem. Eng. J*. **2020**, *387*, 124078. https://doi.org/10.1016/j.cej.2020.124078

(4) Dubascoux, S.; Andrey, D.; Vigo, M.; Kastenmayer, P.; Poitevin, E. Validation of a dilute and shoot method for quantification of 12 elements by inductively coupled plasma tandem mass spectrometry in human milk and in cow milk preparations. *J. Trace Elem. Med. Biol*. **2020**, *49*, 19–26. https://doi.org/10.1016/j.jtemb.2018.04.023

(5) Sun, W.; Roy, A.; Selim, H. M. Residence Time Effects on Molybdenum Adsorption on Soils: Elucidation by Multi-Reaction Modeling and XANES Analysis. *Soil Syst*. **2019**, *3*, 1–14. https://doi.org/10.3390/soilsystems3030055

(6) Krawczyk, M. Determination of macro and trace elements in multivitamin dietary supplements by high-resolution continuum source graphite furnace atomic absorption spectrometry with slurry sampling. *J. Pharm. Biomed. Anal*. **2014**, *88*, 377–384. https://doi.org/10.1016/j.jpba.2013.09.016

(7) Zhang, G.; Zhao, Y.; Liu, F.; Ling, J.; Lin, J.; Zhang, C. Determination of essential and toxic elements in Cordyceps kyushuensis Kawam by inductively coupled plasma mass spectrometry. *J. Pharm. Biomed. Anal*. **2013**, *72*, 172–176. https://doi.org/10.1016/j.jpba.2012.08.007

(8) Wei, Y.; Salih, K. A. M.; Rabie, K.; Elwakeel, K. Z.; Zayed, Y. E.; Hamza, M. F.; Guibal, E. Development of phosphoryl-functionalized algal-PEI beads for the sorption of Nd(III) and Mo(VI) from aqueous solutions – Application for rare earth recovery from acid leachates. *Chem. Eng. J*. **2021**, *412*, 127399. https://doi.org/10.1016/j.cej.2020.127399

(9) Gamal, R.; Rizk, S. E.; El-Hefny, N. E. The adsorptive removal of Mo(VI) from aqueous solution by a synthetic magnetic chromium ferrite nanocomposite using a nonionic surfactant. *J. Alloys Compd*. **2021**, *853*, 157039. https://doi.org/10.1016/j.jallcom.2020.157039

(10) Yadav, A. G.; Gujar, R. B.; Mohapatra, P. K.; Valsala, T. P.; Sathe, D. B.; Bhatt, R. B.; Verboom, W. Highly efficient uptake of tetravalent actinide ions from nitric acid feeds using an extraction chromatography material containing tetra-n-butyl diglycolamide and a room temperature ionic liquid. *J. Chromatogr. A* **2021**, *1655*, 462501. https://doi.org/10.1016/j.chroma.2021.462501

(11) Eriksson, K. E. L. Biotechnology in the pulp and paper industry. *Wood Sci Technol*. **1990**, *24*, 79−101. https://doi.org/10.1007/BF00225309

(12) Ge, Y.; Li, Z. L. Application of Lignin and Its Derivatives in Adsorption of Heavy Metal Ions in Water: A Review. *ACS Sustain. Chem. Eng.* **2018**, *6*, 7181–7192. https://doi.org/10.1021/acssuschemeng.8b01345

(13) Thakur, V. K.; Thakur, M. K.; Raghavan, P.; Kessler, M. R. Progress in Green Polymer Composites from Lignin for Multifunctional Applications: A Review. *ACS Sustain. Chem. Eng.* **2014**, *2*, 1072–1092. https://doi.org/10.1021/sc500087z

(14) Kubo, S.; Kadla, J. F. Lignin-based carbon fibers: Effect of synthetic polymer blending on fiber properties. *J. Polym. Environ*. **2005**, *13*, 97−105. https://doi.org/10.1007/s10924-005-2941-0

(15) Shi, X.; Qiao, Y.; An, X.; Tian, Y.; Zhou, H. High-capacity adsorption of Cr(VI) by lignin-based composite: Characterization, performance and mechanism *Int. J. Biol. Macromol*. **2020**, *159*, 839–849. https://doi.org/10.1016/j.ijbiomac.2020.05.130

(16) Popovic, A. L.; Rusmirovic, J. D.; Velickovic, Z.; Radovanovic, Z.; Ristic, M.; Pavlovic, V. P.; Marinkovic, A. D. Novel amino-functionalized lignin microspheres: High performance biosorbent with enhanced capacity for heavy metal ion removal. *Int. J. Biol. Macromol*. **2020**, *156*, 1160–1173. https://doi.org/10.1016/j.ijbiomac.2019.11.152
(17) Qian, H.; Wang, J.; Yan, L. Synthesis of lignin-poly(N-methylaniline)-reduced graphene oxide hydrogel for organic dye and lead ions removal. *J. Bioresour. Bioprod*. **2020**, *5*, 204–210. https://doi.org/10.1016/j.jobab.2020.07.006
(18) Das, P.; Sharma, N.; Puzari, A.; Kakati, D. K.; Devi, N. Synthesis and characterization of neem (*Azadirachta indica*) seed oil-based alkyd resins for efficient anticorrosive coating application. *Polym. Bull*. **2021**, *78*, 457–479. https://doi.org/10.1007/s00289-020-03120-8
(19) Moawed, E. A.; El-Hagrasy, M. A.; Senan, A. E. A. Application of bio-alkyd resin for the removal of crystal violet and methylene blue dyes from wastewater. *Int. J. Environ. Sci. Technol*. **2019**, *16*, 8495–8504. https://doi.org/10.1007/s13762-019-02343-1
(20) Ifijen, I. H.; Odi, H. D.; Maliki, M.; Omorogbe, S. O.; Aigbodion, A. I.; Ikhuoria, E. U. Correlative studies on the properties of rubber seed and soybean oil-based alkyd resins and their blends. *J. Coat. Technol. Res*. **2021**, *18*, 459–467. https://doi.org/10.1007/s11998-020-00416-2
(21) Wang, Z.; Huang, W.; Bin, P.; Zhang, X.; Yang, G. Preparation of quaternary amine-grafted organosolv lignin biosorbent and its application in the treatment of hexavalent chromium polluted water. *Int. J. Biol. Macromol*. **2019**, *126*, 1014-1022. https://doi.org/10.1016/j.ijbiomac.2018.12.087
(22) Zhang, D.; Xu, W.; Cai, J.; Cheng, S. Y.; Ding, W. P. Citric acid-incorporated cellulose nanofibrous mats as food materials-based biosorbent for removal of hexavalent chromium from aqueous solutions. *Int. J. Biol. Macromol*. **2020**, *149*, 459-466. https://doi.org/10.1016/j.ijbiomac.2020.01.199
(23) Khandelwal, H.; Ravi, B. Effect of molding parameters on chemically bonded sand mold properties. *Journal of Manufacturing Processes* **2016**, *22*, 127–133. https://doi.org/10.1016/j.jmapro.2016.03.007
(24) Galiwango, E.; Rahman, N. S. A.; Al-Marzouqi, A. H.; Abu-Omar, M. M.; Khaleel, A. A. Klason Method: An Effective Method for Isolation of Lignin Fractions from Date Palm Biomass Waste. *Chem. Process. Eng. Res*. **2018**, *57*, 46-58.
(25) Zhai. R.; Hu, J.; Chen, X.; Xu, Z.; Wen, Z.; Jin, M. Facile synthesis of manganese oxide modified lignin nanocomposites from lignocellulosic biorefinery wastes for dye removal. *Bioresour. Technol*. **2020**, *315*, 123846. https://doi.org/10.1016/j.biortech.2020.123846
(26) Xu, X.; Chen, L.; Guo, J.; Cao, X.; Wang, S. Synthesis and characteristics of tung oil-based acrylated-alkyd resin modified by isobornyl acrylate. *RSC Adv* **2017**, *7*, 30439-30445. https://doi.org/10.1039/C7RA02189E
(27) Moawed, E. A.; El-Hagrasy, M. A.; Embaby, N. E. M. Substitution influence of halo polyurethane foam on the removal of bismuth, cobalt, iron and molybdenum ions from environmental samples. *J. Taiwan Inst. Chem. Eng*. **2017**, *70*, 382-390. https://doi.org/10.1016/j.jtice.2016.10.037

SUPPLEMENTARY MATERIAL

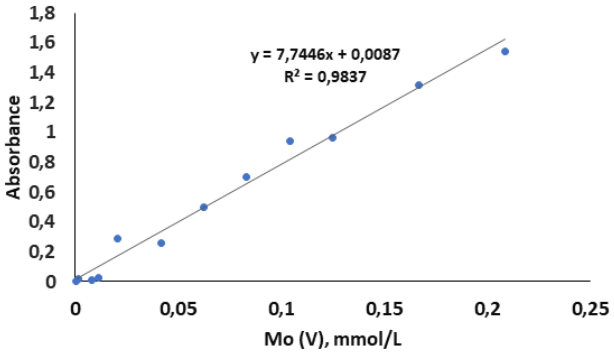

Figure 1S. Calibration curve for determination of molybdenum ions.

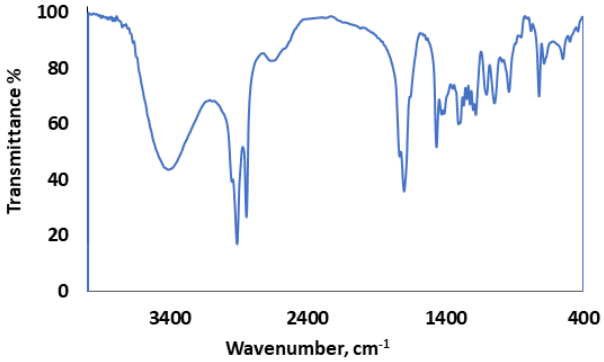

Figure 2S. FTIR spectrum of the A-Resin.

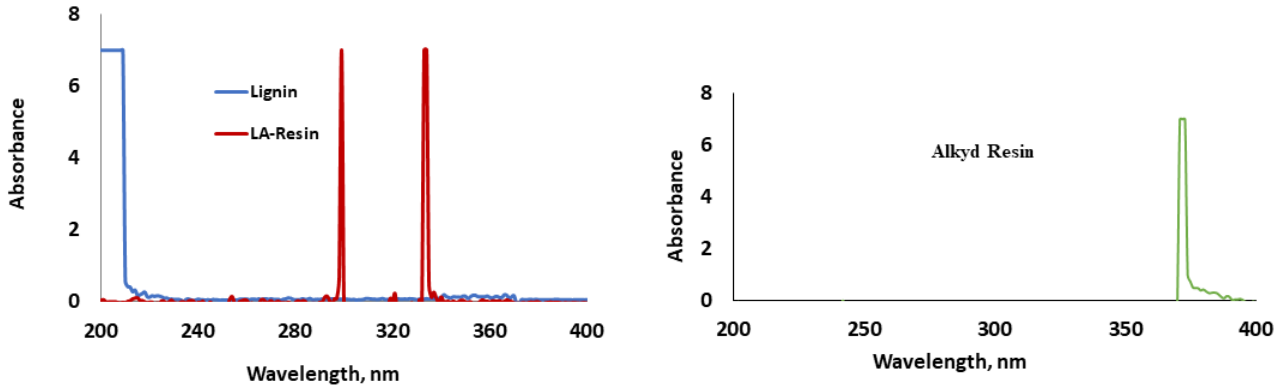

Figure 3S. Electronic spectra for lignin, and LA-Resin.

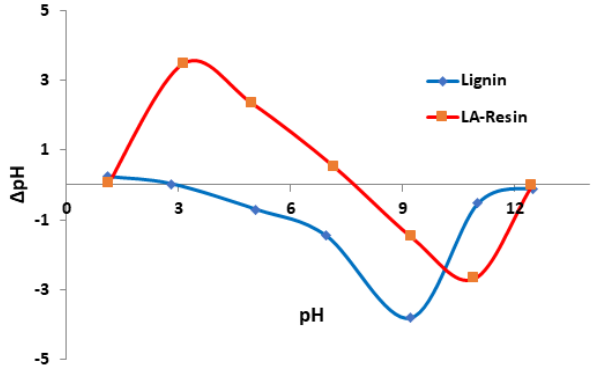

Figure 4S. The pH_{zpc} curves of lignin and LA-Resin.

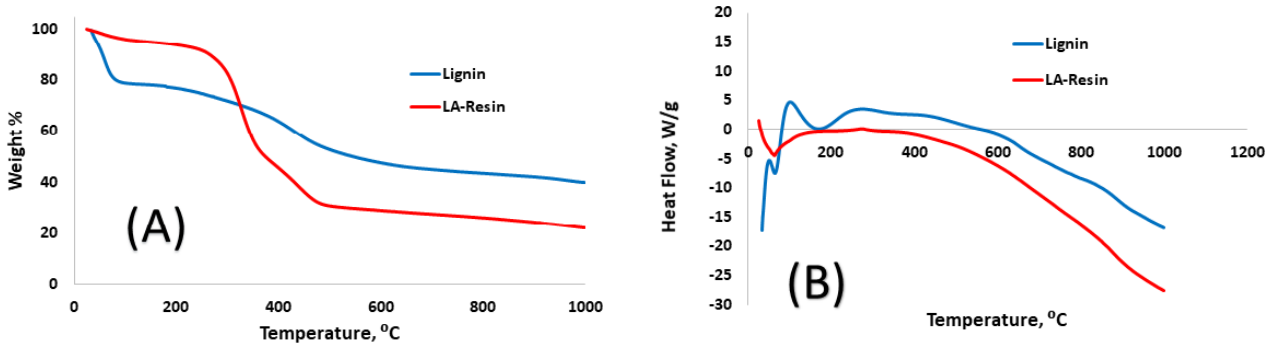

Figure 5S. TGA (A) and DTA (B) curves of lignin and LA-Resin.

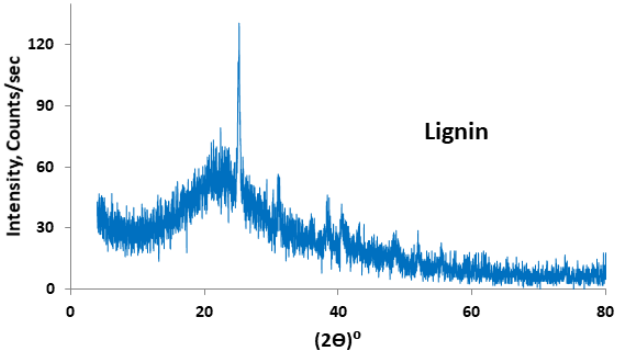

Figure 6S. XRD pattern of lignin.

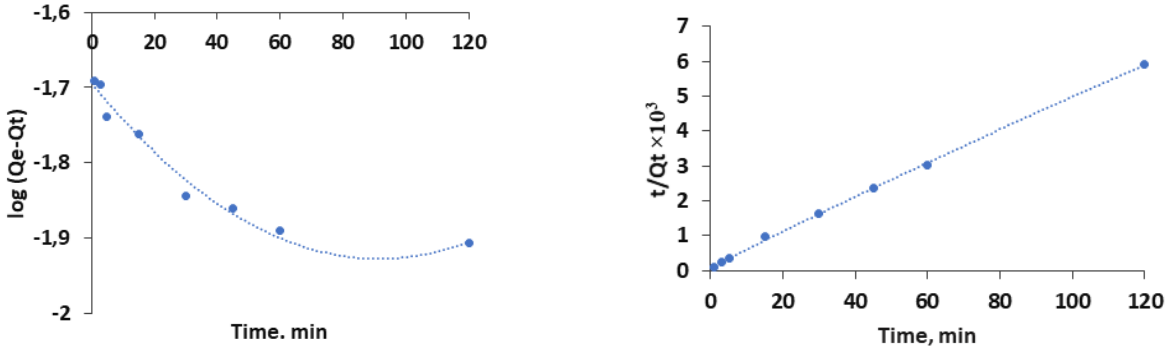

Figure 7S. Plots of non-linear kinetic models for the adsorption of Mo(VI) onto LA-Resin: Initial concentration of Mo(V) ions 5 to 200 mg L^{-1}; amount of LA-Resin 0.1 g; sample volume 25 mL; acidity 1.5 M.

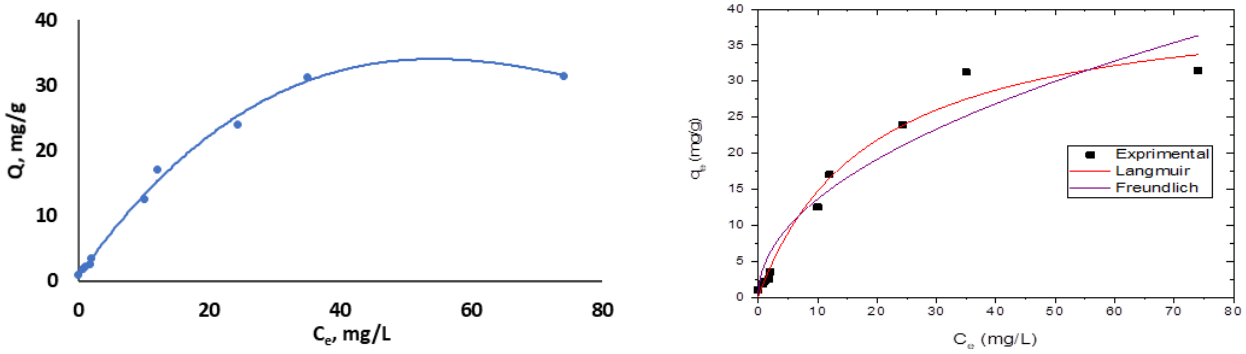

Figure 8S. Plots of non-linear isotherm models for the adsorption of Mo(VI) onto LA-Resin: Initial concentration of Mo(V) ions 5 to 200 mg L^{-1}; amount of LA-Resin 0.1 g; sample volume 25 mL; shaking time 60 min; acidity 1.5 M.

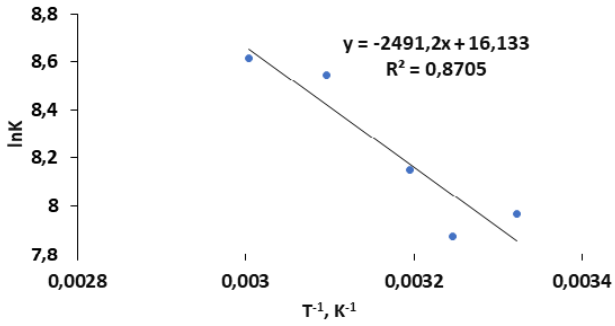

Figure 9S. Plots of thermodynamic model.

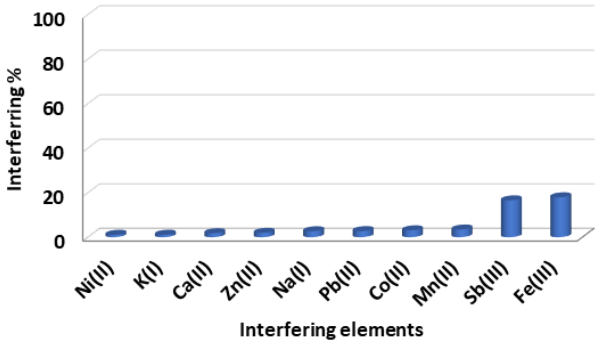

Figure 10S. Effect of the interfering ion on the extraction of Mo onto LA-Resin from aqueous solution.

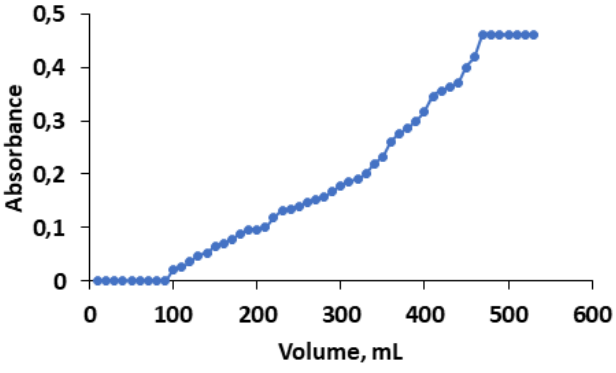

Figure 11S. Breakthrough curve for extraction of Mo from aqueous solution using LA-Resin column.

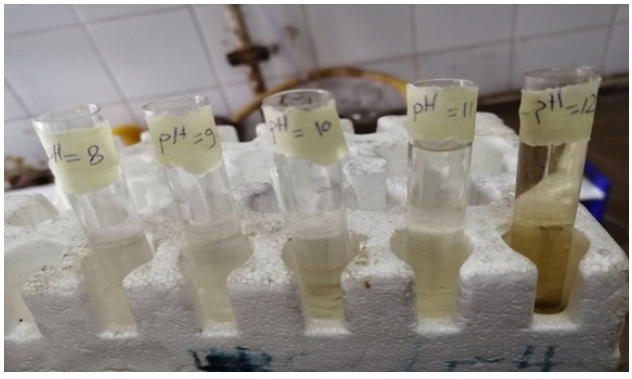

Figure 12S. Effect of alkaline solution on the stability of LA-Resin.

Table 1S. Kinetic and isotherm parameters for the sorption of Mo(V) onto LA-Resin

Kinetics	**Pseudo-first-order model**			**Pseudo-second-order model**		
Parameters	qe_1 (mg g^{-1})	k_1 (min^{-1})	R^2	qe_2 (mg g^{-1})	k_2 (g mg^{-1} min^{-1})	R^2
	1.77	0.043	0.75	1.98	2.01×10^{-5}	0.997
Isotherm	**Langmuir isotherm**			**Freundlich isotherm**		
Parameters	q_{max} (mg g^{-1})	b (L mg^{-1})	R^2	K_F	n	R^2
	39.2	0.026	0.92	0.356	2.01	0.86

*C_o = 8 mg L^{-1}, V = 25 mL, t = 0-120 min, q_{exp} = 1.94 mg g^{-1}

Table 2S. non-linear kinetic parameters for the adsorption of Mo(VI) onto LA-Resin: Initial concentration of Mo(V) ions 5 to 200 mg L^{-1}; amount of LA-Resin 0.1 g; sample volume 25 mL; acidity 1.5 M

Kinetics	**Pseudo-first-order model**			**Pseudo-second-order model**		
Parameters	qe_1 (mg/ g^{-1})	k_1 (min^{-1})	R^2	qe_2 (mg g^{-1})	k_2 (g mg^{-1} min^{-1})	R^2
	1.77	0.043	0.75	1.98	2.01×10^{-5}	0.997

Table 3S. Non-linear isotherm parameters for the adsorption of Mo(VI) onto LA-Resin: Initial concentration of Mo(V) ions 5 to 200 mg L^{-1}; amount of LA-Resin 0.1 g; sample volume 25 mL; shaking time 60 min; acidity 1.5 M

Isotherm	**Langmuir isotherm**			**Freundlich isotherm**		
Parameters	q_{max} (mg g^{-1})	b (L mg^{-1})	R^2	K_F	n	R^2
	42.1	0.053	0.98	4.4	2.2	0.92

Table 4S. Comparison between LA-Resin adsorption capacities of various adsorbents

Adsorbent	**Sorption capacity (mg g^{-1})**	**References**
Ch-NMA	29.7	(1)
Mn_3O_4-TiO_2 nanocomposite	20.6	(2)
WB1000	29.8	(3)
$CrFe_2O_4$ nanoparticles	17.03	(4)
SM-4 resin impregnated with CYANEX 923	8.2	(5)
TVEX- TOPO resin	17.6	(6)
TOA/perlite	7.2	(7)
Brown algae *Laminaria japonica* gel (CAG)	38.19	(8)

(continues on the next page)

Table 4S. Comparison between LA-Resin adsorption capacities of various adsorbents (continuation)

Adsorbent	Sorption capacity (mg g^{-1})	References
Silica gel/quercetin	8.54	(9)
Activated DWTRs	39.2	(10)
NaOCl-oxidized multiwalled carbon nanotubes	22.7	(11)
Di-(2-ethylhexyl) phosphoric acid	25.7	(12)
Carminic acid modified anion exchanger	13.5	(13)
Nano-magnetic $CuFe_2O_4$	30.6	(14)
Chitosan-modified magnetic nanoparticles	35.5	(15)

Table 5S. Thermodynamic parameters for the sorption Mo(V) onto LA-Resin

Thermodynamic parameters		
ΔG (kJ mol^{-1})	ΔH (kJ mol^{-1})	ΔS (J K^{-1} mol^{-1})
-19.2	21.6	137

Table 6S. The values of ΔG at different temperatures

Temperature, K	K	ln K	ΔG
298	2882.653	7.966466351	-19.73749397
308	2629.31	7.874476864	-20.1642674
313	3461.957	8.149589177	-21.20752922
323	5133.929	8.543626448	-22.94324242
333	5516.667	8.615529092	-23.85262645